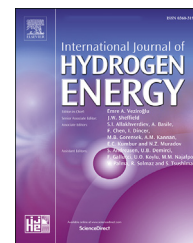




ELSEVIER

Available online at www.sciencedirect.com

ScienceDirect

journal homepage: www.elsevier.com/locate/ijhe

Influence of electrode spacing and fed-batch operation on the maximum performance trend of a soil microbial fuel cell

Meshack Imologie Simeon ^{a,b,*}, Ruth Freitag ^a

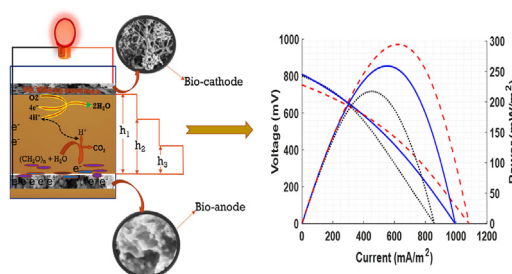
^a Chair of Process Biotechnology, Faculty of Engineering Science, University of Bayreuth, Universitätsstraße 30 FAN-D, 2. Stock, 95447 Bayreuth, Germany

^b Department of Agricultural and Bioresources Engineering, PMB 65, School of Infrastructure, Process Engineering and Technology, Federal University of Technology, Minna, Nigeria

HIGHLIGHTS

- Soil MFC is optimized for efficient substrate utilization and long-term sustainable power generation.
- The effect of long-term fed-batch operation on the MFC performance with varying electrode spacing is investigated.
- Soil MFC performance stability is time dependent on electrode spacing under fed-batch operation.
- Smaller electrode spacing results in initially better performance due to lower internal resistance.
- Larger electrode spacing takes a longer time for the MFC to reach stable and maximum performance.

GRAPHICAL ABSTRACT



ARTICLE INFO

Article history:

Received 16 March 2021

Received in revised form

3 November 2021

Accepted 13 November 2021

Available online xxx

ABSTRACT

The effect of electrode spacing on a soil microbial fuel cell (MFC) performance under fed-batch treatment with synthetic urine medium (SUM) was investigated at 2, 5, and 8 cm electrode spacing. The electrodes consisted of stainless-steel mesh with coarse layers of carbon-black. The MFCs were fed with SUM when the natural substrate of the medium was exhausted. Initial feeding resulted in 79.6, 108.7, and 103.1% increase in OCV with a proportional percentage increase in power at 2, 5, and 8 cm electrode spacing. Six days after the first feeding, the power was 189.9, 150.7, and 108.5 mW/m² in ascending order of

* Corresponding author. Chair of Process Biotechnology, Faculty of Engineering Science, University of Bayreuth, Universitätsstraße 30 FAN-D, 2. Stock, 95447 Bayreuth, Germany.

E-mail addresses: s.imologie@futminna.edu.ng (M.I. Simeon), bioprozesstechnik@uni-bayreuth.de (R. Freitag).

<https://doi.org/10.1016/j.ijhydene.2021.11.110>

0360-3199/© 2021 Hydrogen Energy Publications LLC. Published by Elsevier Ltd. All rights reserved.

Keywords:

Microbial fuel cell
Soil
Electrode spacing
Fed-batch
Maximum performance
Bio-electricity

electrode spacing. With more extended treatment, the overall maximum power was obtained at 8 cm spacing. In ascending order of electrode spacing, the highest power (207.92, 263.38, and 271.1 mW/m²) was obtained on days 39, 42, and 93, respectively. The study shows that a larger anode-to-cathode distance requires a longer time for the soil MFC to achieve stable and maximum performance in fed-batch operation.

© 2021 Hydrogen Energy Publications LLC. Published by Elsevier Ltd. All rights reserved.

Introduction

The adverse effects of the world's dependence on fossil fuels have triggered an intensive search for alternative, environmentally friendly energy sources ([1–3]. Microbial fuel cells (MFCs) have been highlighted in research as a potential component of alternative energy sources because they are natural sources of renewable energy with no harmful emissions [4–7]. The significant challenges to the practical use of MFCs [8] for power generation include microbe-electrode interactions, design issues, and electrochemical limitations [9–11].

Among others, soil or solid anolyte MFCs [12] have a high potential for practical power generation [13,14]. These types of MFCs have attracted research interest because, in addition to generating electricity, they have the unique ability to provide inexhaustible electron acceptors for the oxidation of soil organic pollutants [15]. In addition to being rich in complex sugars and other nutrients that accumulated over millions of years, soil mud forms the natural starting substrates [16] for the growth and maintenance of the activities of the electroactive biofilms (EABs) in MFCs [17]. The soil is rich in a mixed population of bacteria, actinomycetes, fungi, algae, and protozoa [18]. Diverse microbial communities provide high microbial diversity, allowing different substrates to be used in MFCs under non-sterile conditions [19]. The enhanced utilization of substrates in soil microbial fuel cells (S-MFC) may be related to the symbiotic relationship [9] that exists between the mixed microbial population [20]. The complex organic materials such as lignin and cellulose, which are present in the medium and cannot usually be degraded or digested by bacteria, are degraded by the fungi, releasing the simple nutrients for the bacteria to use as substrates [21]. The aerobic microbes in the soil could also benefit the overall microbial electrogenesis by consuming the oxygen surrounding the anode, thus protecting the metabolism of the electroactive anaerobes. As beautiful as these MFC types sound, they suffer a decline in energy production due to increased internal resistance once depleted of their natural substrates [17]. For the long-term application of S-MFCs, it is therefore essential to replenish the substrates after exhaustion. Irregular feeding of an S-MFC (with an anode-cathode spacing of 4 cm) with urine has been reported to improve and stabilize the performance of an MFC [18,19] under various external loads [21]. However, the stability of the MFC with urine as substrate could not be maintained throughout the study period,

probably due to oxygen diffusion into the anode region, which favours the growth of competing aerobes. Similarly, S-MFCs possess catalytic properties in urea degradation in urine and other complex wastewaters. This degradation occurs by ammonification, volatilization, nitrification, and denitrification [22] to yield improved bioelectricity generation [23]. Although soil is an excellent source of electroactive bacteria for MFCs that use synthetic or natural wastewater as a substrate, they are not commonly fed due to their architectural configuration. In a typical S-MFC, the soil acts as a nutrient-rich electrolyte, proton or cation exchange membrane, and source of current-generating microbes such as *Geobacter*, *Sulfurreducens*, *Shewanella*, *Oneidensis* [24,25], and many others [26,27]. The electrodes are configured parallel to each other. The cathode is in constant contact with oxygen. It is placed some distance above the anode (buried in the soil to maintain an anaerobic condition) to create a natural potential. Continuous substrate feeding in such a system is limited. Therefore, a fed-batch operation is necessary to keep nutrients from becoming a limiting factor and to continue to draw maximum power from it. Theoretically, an S-MFC can produce electricity endlessly as long as the reactor conditions remain favourable for electricity production by the electrode-associated microbes [15,28]. This potential makes them attractive candidates for developing sensors for remote sensing of environmental pollution [18,19]. However, a suitable electrode spacing must be found to minimize the effects of fouling, plugging, and oxygen concentration at the anode that occurs during long-term operation of single-chamber MFCs with wastewater as substrate [21,30].

The parameters of the MFC system design, such as electrode properties and spacing, influence the formation and efficiency of electron transfer from electroactive biofilms [25]. In many cases, the power output of MFCs is inversely proportional to the anode-cathode interval due to a reduction in Ohmic resistance and efficient charge transfer between the electrodes at smaller electrode spacings [30–32]. This trend may not apply to S-MFCs on a continuous or fed-batch operation. A too-small anode-cathode spacing may result in high oxygen availability at the anode. This would promote the growth of aerobes around the anode, and competition for available nutrients would reduce the activity of the EABs, resulting in a down-trend performance. Besides, a too-small anode-cathode distance in the absence of a separator can lead to a short-circuit [33,34] as the electrolyte conductivity

increases. On the other hand, larger electrode spacing can minimize clogging and fouling, thus improving power density during the long-term operation of MFCs [30]. However, a too large anode-cathode distance can lead to a slow mass transport through the mud, limiting substrate availability at the anode. Oxidation of the substrate at the anode results in electrons generation and transportation through an external load to the cathode, where electron acceptors such as oxygen and nitrogen are reduced. This transport phenomenon induces charge movement across the proton or cation exchange membrane to maintain the charge balance of the system. In S-MFC, the mud, which is the source of the bacteria and electrolyte, also acts as the exchange membrane. Therefore, in an S-MFC using a complex substrate, a too-large electrode space may limit the transport of protons, mainly hydrogen (H^+) or H_3O^+ and other cations (such as K^+ , Na^+ , Ca^{2+} , NH_4^+ , and Mg^{2+}) [35] towards the cathode [36]. This leads to increased diffusion resistance and consequently to a decrease in power generation [37]. Thus, too small or too large an electrode gap has a negative effect on the electrocatalytic potential of the EABs, leading to a decrease in the power density of the S-MFCs. Therefore, there is a need to optimize the electrode spacing of the S-MFCs for efficient long-term substrate utilization and maximum power generation.

Most previous studies on S-MFCs were designed and operated with arbitrarily chosen anode-cathode spacing [12,14,15,19,21,38–41]. For example, Li et al. [15] demonstrated the in-situ representation of soil conductivity by electrochemical impedance spectroscopy using Keego Technology's MFC kits with an electrode spacing of 3 cm. The same kits were used to investigate the influence of external loading and utilization of urine in S-MFCs with an electrode spacing of 4 cm [17,18,21]. Urine was found to significantly improve performance due to a reduction in losses and an improvement in the conductivity of the bulk electrolyte. However, the performance deteriorated slightly over time due to the increased oxygen concentration in the anodic region. In a similar study, Barbato et al. [39] also used Keego Technology's MFC to investigate the performance of S-MFC at different temperature regimes and an anode-cathode distance of about 3 cm. Using a similar MFC configuration, Pietrelli et al. [38] developed a wireless sensor network driven by an S-MFC with an electrode spacing of 8 cm. Since these studies were carried out with different objectives, the influence of the electrode spacing under substrate supply was not considered.

The effects of electrode spacing on the short-term performance of a soil MFC in batch feeding have been reported previously [42]. However, the long-term effects of extended feeding have not been reported. It is unknown how close the electrodes can be spaced in a fed-batch operation [30] of an S-MFC. Therefore, this study, an extension of work recently presented at a conference [43], investigates the possibility of extracting sustainable and implementable maximum power from a soil-based MFC. The effect of substrate feeding at a regular interval and different electrode spacing on the stability and long-term performance of the MFC was investigated. The overall goal is to find the best electrode spacing at which maximum power can be extracted from S-MFC for real-world application for an extended operating period without the need to change the medium or the electrodes regularly.

Materials and methods

Construction of MFCs reactors and electrodes

The MFC reactors were built in the glass workshop of the University of Bayreuth, Germany. Each reactor consisted of a screw cap with holes to connect the current collectors and an adjustable 6 mm tube for proper cathode ventilation and for holding the cathode securely in place. The cylindrical reactor was made of glass with a port at the bottom next to the anode position for substrate sampling and anode pH and conductivity measurement. All vessels were designed with a diameter of 78 mm, but with different heights (60, 90, and 120 mm) to accommodate the electrode spacings.

All electrodes (both anodes and cathodes) were made from the same materials, with stainless steel (SS) serving as the base material. Each electrode was coated with a layer of highly conductive carbon black (CB) (Vulcan XC 72, Keego Tech, Texas) on a stainless-steel wire mesh (type 1.4301, Germany, with a mesh size of 0.315) with a two-component epoxy binder (UHU plus ENDFest, Germany). The coating was necessary to increase the specific surface area for biofilm attachment [43–45] and long-term stability [46]. Epoxy was used as the binder due to its better adhesive properties and long-term stability in the S-MFC system than other polymer binders, which were preliminarily studied (results not shown here). To improve the electrical properties of the binder, it was prepared by mixing 1:1 (2.7 g each) of the two components epoxy with about 0.26 g CB. The mixture was mechanically homogenized into a paste by manual stirring. The paste was applied evenly to both sides of the SS wire mesh (diameter of 6.5 cm and circular cross-sectional area of 33.18 cm²). More CB was then applied evenly to both sides, clamped between two planes, and left overnight at room temperature (20 °C ± 0.5 °C) to form correctly before use. The SS was cut so that a strip of it remained to create a connector, connecting the electrode to an external circuit and data acquisition systems. Each connector was insulated with heat shrink tubing (Ø 0.50–0.25 cm) using a heat gun at 120 °C.

Soil sampling and preparation

Topsoil (10–20 cm below ground surface) and garden compost were collected from the botanical garden of the University of Bayreuth, Germany. A mixture of an equal amount of the soil contained 56.82% sand, 13.64% silt, and 29.54% clay as determined with standard methods before sieving. The conductivity, pH, and moisture content of the soil mixture were 2.23 mS/cm, 6.73, and 26.15%. The pH and conductivity were measured by Groline soil testers (HI981030 and HI98331, Hanna Instruments, Germany), while the moisture content was determined with the standard oven method. An equal amount of these soil types was sieved through a 2 mm SS sieve to remove plant debris and other earth leaves and then homogenized by mixing with a stainless-steel spatula [47] before use. A mixture of the two soil types was used because, based on our previous studies [43,44], the combination gives good porosity for substrate availability at the anode. The homogenized soil mixture was saturated with de-ionized water [40] to

obtain mud that served as the nutrient-rich natural medium, the source of bacteria, and the cation exchange membrane [21] for the MFCs.

MFCs setup and operation

Each MFC (Fig. 1) was constructed by adding approximately 1 cm of mud (about 90 g) to the bottom of the MFC vessels before installing the anode. Additional mud (136 g, 385 g, and 620 g for 2 cm, 5 cm, and 8 cm cathode-anode spacing, respectively) was applied to the anode. Then the cathode was installed so that there was a gap of approximately 40 mm between the cathode and the lid to allow good ventilation of the cathode. The reproducibility of the results was tested by evaluating the performance of the MFCs through 2 successive series of experiments with the same setup and each time with new electrodes and mud. The MFCs were operated at ambient temperature (20 ± 0.5 °C).

Open-circuit voltage (OCV) was recorded every hour through a data logger (ADC-24, Pico Technology) to monitor the growth of the electroactive biofilm. The data logger was paused whenever a Potentiostat was used for electrochemical data acquisition. After a stationary growth phase was reached and a decline in voltage was observed, suggesting the exhaustion of the natural substrate of the medium, SUM was injected into the cells as substrate. This marked the first point of feeding. The components of the SUM were selected to mimic urine [48]. They consisted mainly of urea and sodium chloride with traces of other elements as follows: 15 g/l of Urea ($\text{NH}_2(\text{CO})\text{NH}_2$), 5.2 g/l of NaCl, 0.5 g/l of Uric acid ($\text{C}_5\text{H}_4\text{N}_4\text{O}_3$), 0.8 g/l of Creatinine

($\text{C}_4\text{H}_7\text{N}_3\text{O}$), 0.1 g/l of Lactic acid ($\text{C}_3\text{H}_6\text{O}_3$), 2.1 g/l of NaHCO_3 , 0.7 g/l of NH_4Cl , 1.2 g/l of K_2HPO_4 , 0.2 g/l of $\text{MgSO}_4 \cdot 7\text{H}_2\text{O}$, 0.95 g/l of KH_2PO_4 , 1.80 g/l of Na_2SO_4 and Millipore water was added to make the volume up to 1 L. Following an earlier study [18], the substrate was added at six (6) day intervals throughout the study period after the initial substrate addition. While a single setup for each electrode spacing was used in the first experiment, duplicates were used in the second. Each MFC was fed with 10ul/g of mud [43]. The MFCs were operated for 102 days, which is sufficient time to study their long-term performance stability [49].

Electrochemical measurement

Polarization and power density curves were determined by linear sweep voltammetry (LSV) using a potentiostat (VMP3 Biologic Science Instruments, France). For LSV, a two-electrode system was used with the anode as the working electrode and the cathode as the reference and counter electrode. Each polarization experiment was performed at a scan rate of 1 mV/s by lowering the MFC voltage from OCV to 0 V [37,50], and this was repeated every three days to track the maximum performance of the MFCs. The OCV, theoretical current, theoretical power, maximum power, fill factor, voltage, and current at maximum power, and internal resistance were determined from each polarization sweep. The total internal resistance was calculated using Ohms law from the current and voltage parameters at the maximum power point (MPP) ($R = V/I$, where R = resistance, V = cell voltage, and I = current). Electrochemical impedance spectroscopy (EIS) was performed on a full-cell basis at open-circuit potential and a frequency range of 100 kHz to 10 mHz and an amplitude of 10 mV.

Sample preparation for biofilm imaging

At the end of the experiment, each anode of the MFCs was cut into smaller pieces (1 cm^2). The samples were carefully rinsed in distilled water to remove non-adherent dirt particles. They were then technically fixed with 2.5% glutaraldehyde in 0.1 M phosphate buffer (pH 7.2) overnight at 4 °C, washed in de-ionized water, and dehydrated by successive immersion in a series of ethanol solutions of increasing concentration (30%, 50%, 70%, 80%, 90%, and absolute ethanol) for 10 min [51] and air-dried overnight at room temperature [52]. The samples were spotted with platinum and imaged using a field emission scanning electron microscope (Zeiss Ultra Plus) at the Bavarian Polymer Institute (BPI), Bayreuth, Germany.

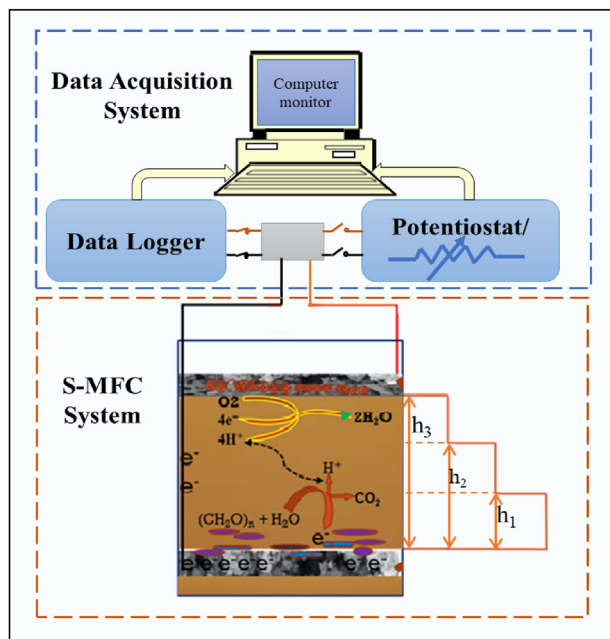


Fig. 1 – Schematic diagram of the MFC setup, the bio-electrochemical reaction of the S-MFC, and data acquisition system. For electrode spacings h_1 , h_2 , and $h_3 = 2, 5,$ and 8 cm , respectively, the MFCs are denoted as MFC_2 h, MFC_5 h, and MFC_8 h.

Results and discussions

The results of the first series of experiments were already presented [43]. Therefore, this report focuses on the outcome of the second series of experiments. Where necessary, reference is made to the first experiment. The results are presented as averages of the performances of a pair of MFCs for each electrode spacing. When significant differences were observed during the long-term operation, results are represented separately to explain the observed effect.

Effect of initial feed on the MFCS performances

Fig. 2 presents the performance curves of the MFCs before and after the initial feed.

The power parameters extrapolated from Fig. 2 are shown in Table 1. Before treatment, the MFC_2 h, MFC_5 h, and MFC_8 h had OCVs of 432, 380, and 390, respectively, with corresponding maximum powers of 51.54, 30.44, and 23.3 mW/m². Six days after treatment, OCVs increased by 79.6, 108.7, and 103.1%, with a proportional percentage increase in power (Table 1). The better performance of MFC_2 h at the same OCV (787 + 7.8 mV) compared to the other MFCs after treatment is not an anomaly because its internal resistance was lower due to a smaller electrode spacing. This observation is consistent with the general trend of MFC performance. Shorter electrode spacing ensures immediate substrate availability at the anode, enhances microbial metabolism, and increases charge transfer from the EABs to the anode, leading to better performance.

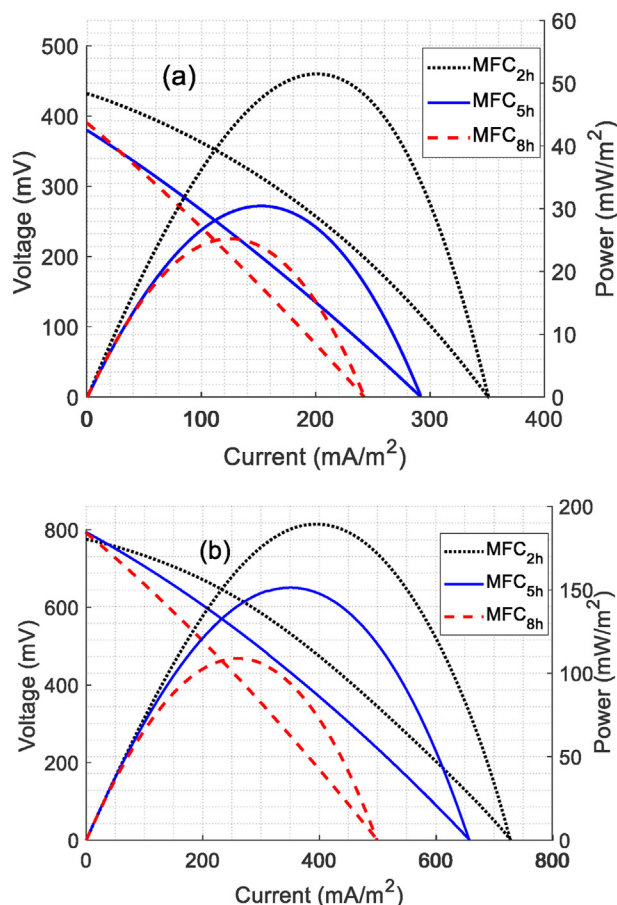


Fig. 2 – Effect of initial feeding. (a) The power curves were obtained from linear sweep voltammetry performed on day 15 before the initial injection (feeding) of SUM into the MFCs. **(b)** power curves were obtained on day 21, just before the second feeding. The Polarization sweep was carried out between open-circuit and zero potentials to estimate the efficiency (fill factor) of the MFCs.

effect of continuous feeding on the long-term stability of the S-MFCs performance

The performance of the MFCs in terms of hourly OCV profile, OCV, and power density obtained with LSV every three days and a representation of the power density of MFC_5 h and its duplicate are shown in Fig. 3. This representation was deemed necessary because an apparent loss of power occurred at some points with this electrode spacing and resulted in large standard deviations.

The MFCs were fed on day 15 when a slight drop in performance was first observed. All MFCs responded positively to this first feeding, as observed between days 15 and 21. The subsequent two consecutive injections of the substrate resulted in an exponential increase in OCV and performance before stabilizing around day 30. At 2 cm spacing, the MFC produced stable OCV and power of 787 ± 25 mV and 202 ± 4 mW/m², respectively, for 15 days between days 30 and 45. After that, an exponential decrease in power was observed. A 63% decrease in OCV resulted in an 83.6% reduction in power density between days 45 and 54. Subsequent feeding did not improve performance at this electrode spacing, but stable OCV and power of 269.3 ± 27 mV and 33.9 ± 4.2 mW/m² were recorded. The sudden shift in stability position of MFC_2 h from a higher to a lower level can be attributed to an increase in the activities of the less electroactive microbial community, most likely aerobes due to the rise in oxygen concentration at the anode during long-term feeding [21].

Fig. 4 compares the change in the internal resistance of the MFCs with time.

The internal resistances in Fig. 4 also represent the resistance at which the maximum powers were measured since, according to the theorem of maximum power transfer, the sum of all internal resistances is equal to the external resistance at MPP. An increase in internal resistance (R_{int}) was initially observed at all electrode spacings during the lag phase when microbial activity was lowest. As shown in Fig. 4, increased microbial activity due to substrate availability decreased internal resistance and thus improved performance. When a total or partial loss of power was observed, the internal resistance also increased dramatically. The points where total power loss occurred are outliers (see the supporting document (Sup. 2 and 3) and omitted from Fig. 4 to clarify the temporal changes of internal resistance of the MFC at different electrode spacing.

Fig. 5(a) shows that MFC_5 h and MFC_8 h showed better performance in extended fed-batch operation. MFC_5 h produced a maximum power density of 263.38 ± 4.5 mW/m² at a current density of 561 ± 9.6 mA/m² on day 42, while MFC_8 h produced 271.1 ± 11.3 mW/m² at a current density of 600.4 ± 23.1 mA/m² on day 93. From the trends of maximum performance (Figs. 2 and 3), it can be inferred that initially, better performance was obtained with the smaller electrode spacings due to lower internal resistance (Fig. 4). Between day 9 and day 30, MFC performance was best with a spacing of 2 cm; between day 30 and day 69, a spacing of 5 cm produced the best performance, and after that, an electrode spacing of 8 cm was best. This reversal of the trend over time can only be explained

Table 1 – Maximum performance indices^a of the MFCs before and after the first feed.

Before Substrate feeding				After initial Substrate feeding		
MFC	MFC_2 h	MFC_5 h	MFC_8 h	MFC_2 h	MFC_5 h	MFC_8 h
I _{sc} (mA)	1.17	0.97	0.81	2.42	2.18	1.66
E _{oc} (mV)	432	380	390	776	793	792
PT (mW/m ²)	150.85	111.51	93.43	563.6	521.4	394.8
P _{max} (mW/m ²)	51.54	30.44	23.3	189.9	150.7	108.5
I _{opt} (mA)	0.67	0.51	0.41	1.32	1.17	0.86
V _{opt} (mV)	255.8	198.4	202.6	477.3	430.4	419
R _{int} (Ω)	383.1	389.8	490.4	361.6	367.9	487.2
FF (%)	34	27.4	26	33.5	29	27.5

^a I_{sc} = short circuit current, E_{oc} = open circuit potential, PT = theoretical power, P_{max} = maximum power, I_{opt} = current at maximum power, V_{opt} = voltage at maximum power, R_{int} = internal resistance, and FF = fill factor (theoretical efficiency).

by extended feeding. Therefore, it is necessary to find the right feeding rate to continue to draw maximum performance from an S-MFC at lower electrode spacing. The proportionality of the time for the best performance of the MFCs to the electrode spacing (Fig. 5(b)) suggests that the anode-cathode spacing in this design limited the immediate substrate availability at the

anode, while the extended feed negatively affected the maximum performance at smaller electrode spacings.

More extended stability of the OCV was observed at electrode separations of 5 cm and 8 cm (Fig. 3(C)). Although the OCV gives an idea of the thermodynamic potential of the MFC due to the redox reaction and metabolic activity of the EABs, it

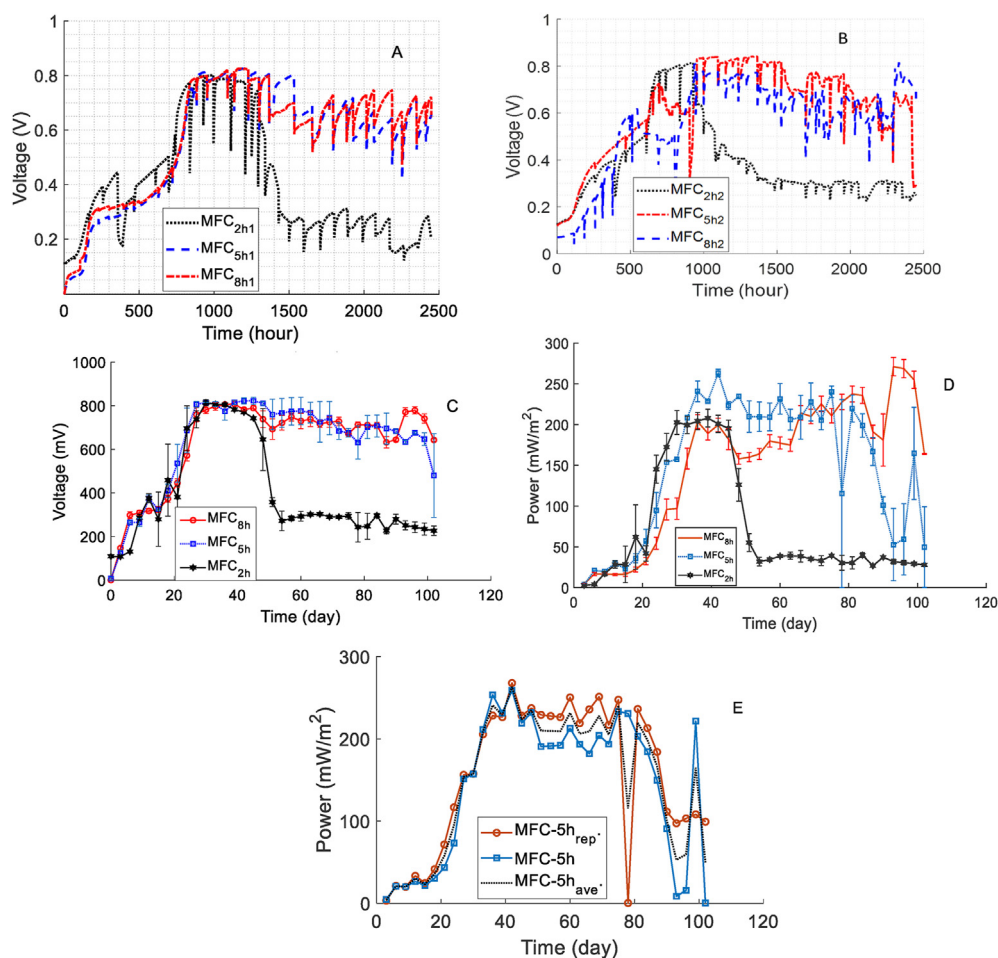


Fig. 3 – Long-term performance trend of the MFCs: A) and B) hourly OCV profile of the MFCs and duplicates measured with ADC-24. The depressed points mark the point of polarization. C) Average OCVs measured with a potentiostat during LSV. D) Maximum power tracking of MFCs as a function of time. E) Power variation of MFC_5 h and its duplicate showing points of power loss. The data points represent the mean, while the error bars represent the standard deviation calculated from the performance of duplicate MFCs with the same electrode spacing.

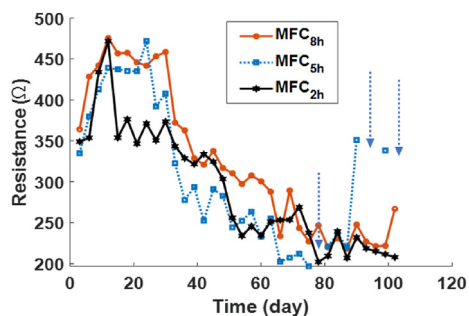


Fig. 4 – Variation of total internal resistance with time. The missing data points indicated by arrows are omitted outliers. The internal resistance was calculated with the current and voltage parameters of the MPP during polarization.

does not consider the charge transfer and diffusion kinetics in the system because there is no current flow in the absence of an external load. Therefore, the intermittent power losses observed at some points during long-term fed-batch operation (Fig. 3(E)) are not evident in Fig. 3(C). These losses were essentially observed after three days of feeding. This loss could have occurred earlier, but the polarization sweep was performed every three days to allow the MFCs to recover after each cycle of polarization.

The occasional loss of power was more pronounced at 5 cm electrode spacing. On day 90, 90.6% loss of power density was observed in MFC_5 h, due to a 91.1% decrease in current production than the previously measured current (Fig. 5(c)). This loss was followed by an 88.1% increase in current, leading to a power recovery on day 99. A similar observation was also made with the duplicate MFC_5 h. It is worth noting that this phenomenon was mainly due to loss of current and increase in internal resistance, with no significant change in OCV (Fig. 5(b)). The current drop was proportional to the cell voltage only for the last energy loss of the MFC_5 h duplicate. Although this power loss-recovery cycle was also observed at 8 cm electrode spacing due to current loss, no complete energy loss was recorded. The maximum power loss at this spacing was 55.5% on day 102.

After the loss, this self-recovery of the initial energy level suggests a switch between two opposing metabolic processes, possibly by the same or similar microbial community. The same cell voltage implies microbial communities with the same electrochemical redox potential. In contrast, the energy loss suggests a microbial preoccupation with activities other than electron transfer (lack of electron transfer from EABs to electrodes). As evidenced by the loss of current, the drastic reduction in the electron transfer response may be attributed to the degradation (hydrolysis and fermentation) of the complex synthetic substrate or other organic compounds accumulated in the system as a result of continuous feeding. The anodic pH value of the MFC was relatively stable at 6.9 ± 0.3 , while the pH value at the cathode was 7.63 ± 0.35 before the power loss. A sudden rise in cathodic pH from 7.54 (before the power loss) to 8.70 (at the power loss) was recorded. The pH of the anode and cathode measured on the last day are

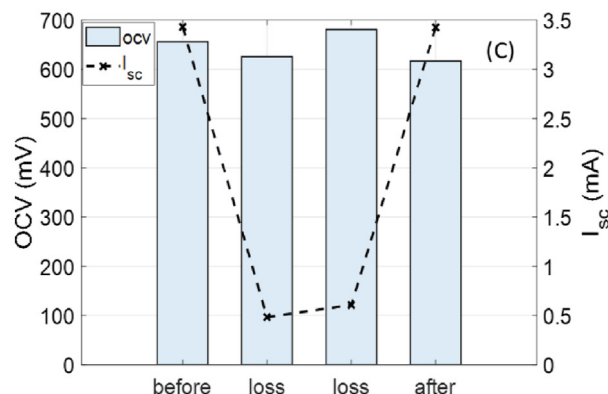
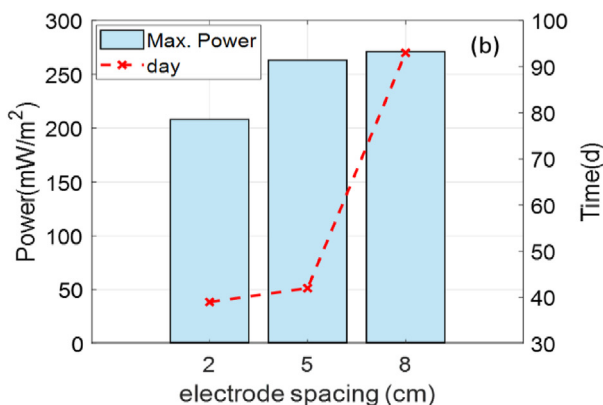
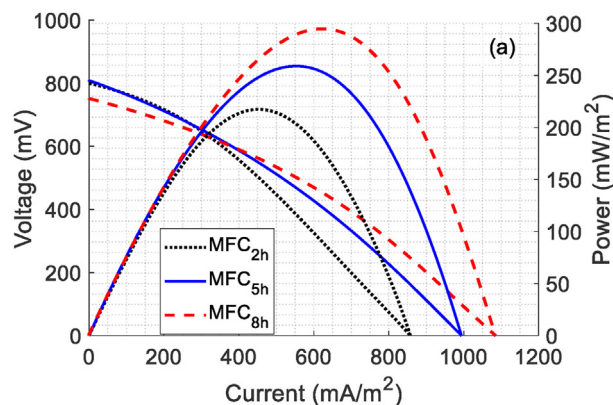
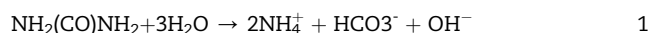


Fig. 5 – (a) Best performance curves of the MFC at different electrode spacings. (b) Best performance at different electrode spacings and the corresponding days. (c) Open-circuit voltage (OCV) and Short-circuit current or limiting current (I_{sc}) were measured at 5 cm electrode spacing on day 90 (before), days 93 and 96 (during), and day 99 (after) power loss.

presented in the supplementary document (Sup.1). Hydrolysis of urea in urine results in an increased pH of the bulk electrolyte due to the conversion of neutral urea to charged compounds [53] according to Eq. (1).



The organic compound was presumably further degraded by the bacterial cells after hydrolysis through fermentation,

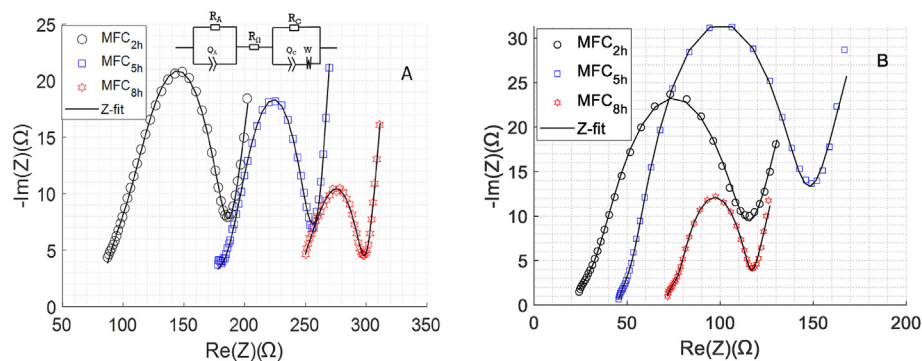


Fig. 6 – The Nyquist impedance of the MFCs: A. day 30, B. day 90. The charge transfer and diffusion characteristics shown in Table 2 were obtained by simulating the EIS spectra with an equivalent electrical circuit (Inset in Fig. 6(a)).

Table 2 – Impedance and kinetic characteristic of the MFCs.

Initial EIS							
spacing	R_{Ω}	R_{ct} (Ω)	C_{dl} (F)	Q (F.s(a-1))	b	W (Ohm.s ^{-1/2})	
2	87.14	110.96	1.34E-04	1.29E-03	0.3199	4.417	
5	177.8	82.65	2.18E-04	1.17E-03	0.3469	4.752	
8	250.3	59	1.28E-04	1.54E-03	0.3486	3.193	
Final EIS							
2	24.16	95.02	3.29E-04	3.84E-03	0.2944	4.798	
5	46.27	100.4	4.59E-04	8.94E-04	0.5975	4.493	
8	71.72	46.13	4.27E-06	8.45E-04	0.7187	3.407	

R_{Ω} is the Ohmic resistance, Q = constant phase element denoted as Q_a and Q_c for anode and cathode, respectively, in the equivalent circuit; b is the coefficient of Q , W is the Warburg impedance coefficient. R_{ct} was obtained by adding R_a (anodic charge transfer resistance) and R_c (cathodic charge transfer resistance) in the circuit since EIS was measured on a full-cell basis.

resulting in volatile fatty acid production consumed by anode-breathing bacteria or methanogenic *Achaea*, leading to the release of electrons at the anode [54]. Thus, the power increased to the initial value after hydrolysis and fermentation. Since this energy loss was not evident in the early stages of the feeding cycles, continuous feeding may have increased the substrate's complexity resulting in the synthesis of untargeted end-products (such as methane) by the activities of methanogens [55,56]. Kumar et al. [22] reported that an MFC built with a mixture of compost soil and urea exhibited multifunctional performance characteristics by producing hydrogen and electricity in addition to cleaning the environment. The recovery of ammonium with simultaneous electricity generation from compost soil MFC and urine has also been reported [23,35,57]. Therefore, this power loss may have resulted from converting electrical energy into other useful energy that was not harnessed in this study. Further studies are needed to gain more insight into the cause of this energy loss-recovery phenomenon. Therefore, the MFCs were destructively sampled at the end of the experiment to investigate the components of the microbial communities (results not presented here).

Impedance spectroscopy of the MFCs

The impedance spectroscopy of the MFCs at the beginning of the steady-state (day 30) performance and final EIS measured on day 90 are shown in Fig. 6.

The ohmic resistance of MFCs is theoretically proportional to the electrode spacing [8]. This trend is also true for the MFCs in this study. The ohmic resistance (R_{Ω}) from the initial and final EIS is proportional to the electrode spacing. However, this is not true for the charge transfer resistance (R_{ct}) and double-layer capacitance (C_{dl}). Although the ohmic resistance of MFC_8 h was higher than the other two MFCs, it had the lowest R_{ct} and C_{dl} . These parameters are a function of biofilm properties. The higher R_{ct} and C_{dl} at 2 cm and 5 cm electrode spacing indicate an increase in the size of the anodic biofilm, probably due to increased activities of competing non-electroactive microbial communities or electrode fouling at lower electrode spacings. The EIS spectra obtained at some points where the MFC-5h suffered a total power loss are given in the supplementary document (Sup. 2 and 3) The large R_{ct} (about 100 k Ω) obtained from the diameter of the semicircle and the absence of Warburg behaviour shows that the performance of the MFC was limited by charge transfer and not by diffusion kinetics. This is consistent with the LSV result, which showed that most of the power loss was due to current loss without significant change in voltage. Therefore, the increase in internal resistance observed at a distance of 5 cm was due to increased R_{ct} , which is related to biofilm activities. This result confirms that the observed power loss is due to a decrease in the electroactivity of the bacterial consortia and not to the contact resistance since there was no increase in ohmic resistance. The ohmic resistance is composed of the contact

resistance, the electrodes' resistance, and the bulk electrolyte's resistance [45,50].

surface morphology and biofilm structure of the electrodes

The SEM micrographs of selected electrodes before and after use are presented in Fig. 7. A close examination of the anodic biofilm shows rod-shaped structures linked with nanowires. The cathodes show well-structured, widespread biofilms and interconnected microbial nanowires such as the electrically conductive appendages produced by some bacteria, particularly (but not exclusively) by the genera *Geobacter* and *Shewanella* [25]. Identification of spherical-shaped microbial biofilm was difficult because the electrodes were made of a mixture of coarse and nano-porous materials of sizes between 20 and 100 nm.

The structure of the cathodic biofilm (Fig. 7(E)) reveals the presence of cross-linked microbial pili with possible direct electrode transfer over long distances from one species to another and the electrode. This is an indication that microorganisms catalyzed the oxygen reduction reaction at the cathode. Therefore, the cathode of an S-MFC can be

called a self-developed biocathode. The biocathode has been linked with enhanced and sustainable bioelectricity generation. This is because cathode-associated microbes can oxidize transition metals and provide electrons for oxygen reduction catalysis [58,59]. In contrast, however, long-term operation of biocathodes in wastewater-fed MFCs leads to fouling, which results in reduced oxygen reduction potentials of the cathode and consequently reduced power density [53]. The SEM images of the cathodes shown in Fig. 7 (F and G) exhibit fouling. Liu et al. [30] reported that clogging and fouling due to bacterial accumulation on the electrodes could be prevented with a larger electrode spacing. This explains why better performance was obtained with a longer operating time with an electrode spacing of 8 cm. Therefore, long-term fed-batch operation of the S-MFCs in this study had a more substantial negative effect at smaller electrode spacing.

Preliminary implementation of the MFCs

This study aimed to optimize the S-MFC for possible long-term practical use in developing environmental sensors and

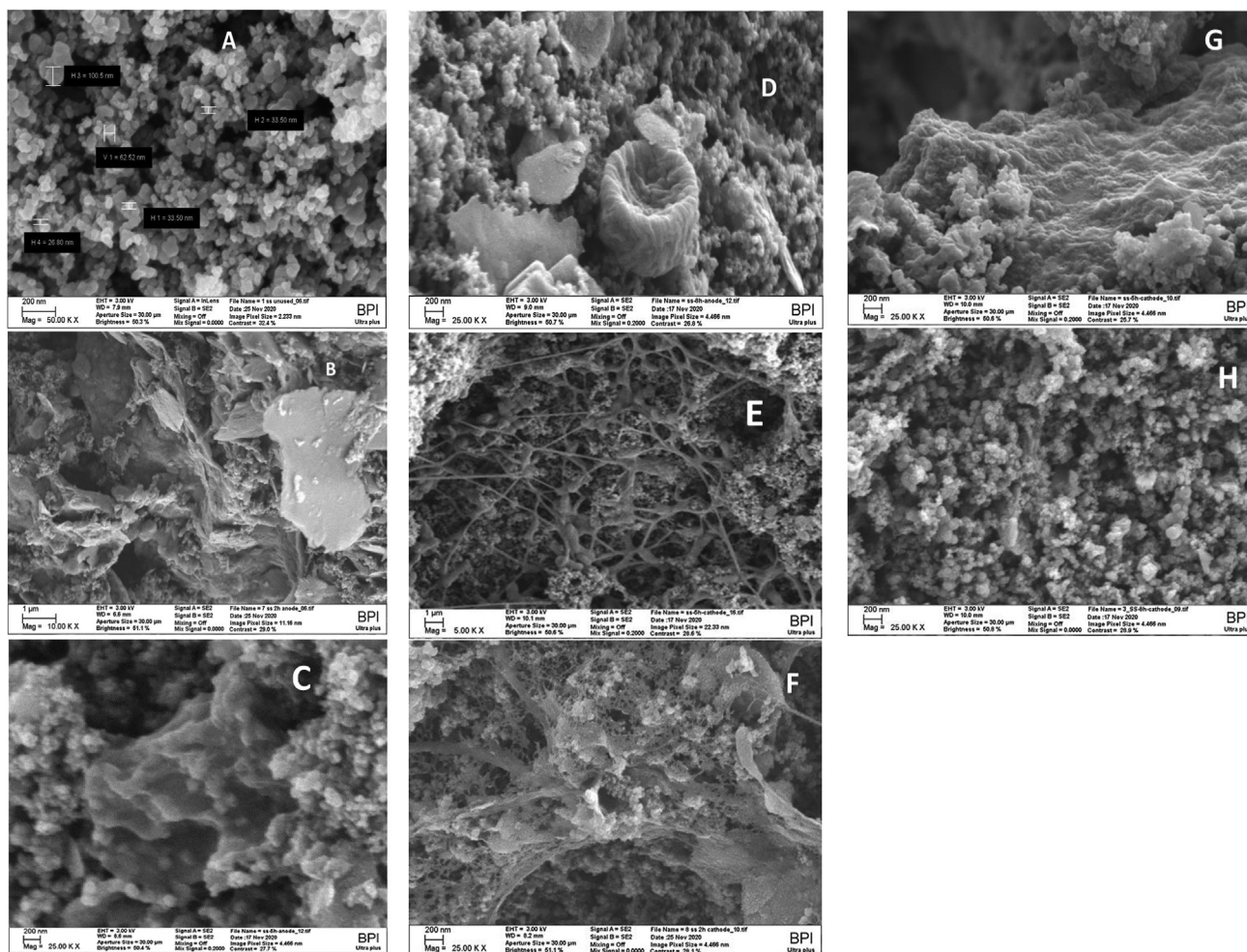


Fig. 7 – SEM Micrographs: (A) unused electrode; (B) MFC_2 h anode; (C) MFC_5 h anode (D) MFC_8 h anode, (E) MFC_5 h cathode with interconnected microbial nanowires, (F) MFC_2 h fouled cathode, (G) MFC_5 h fouled cathode, (H) MFC_8 h cathode.

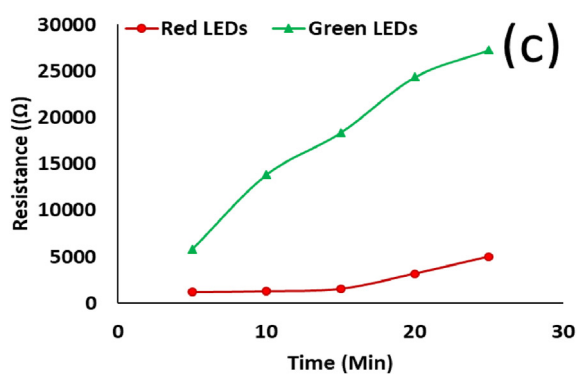
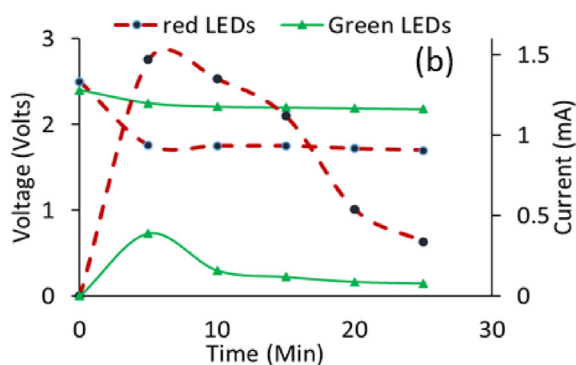
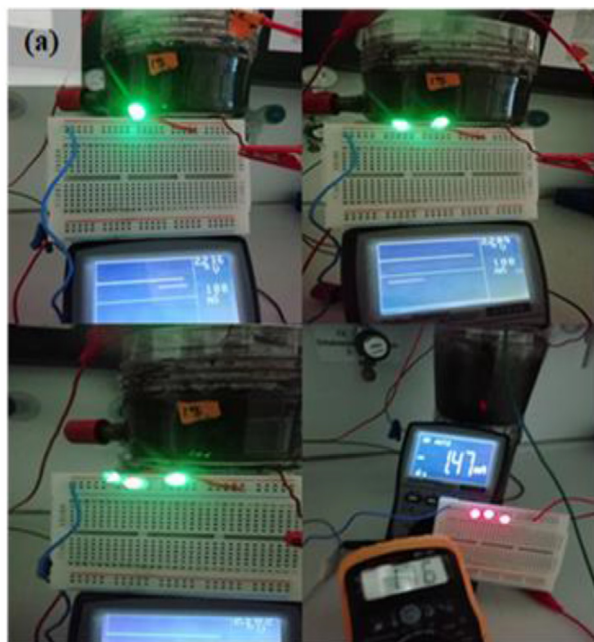


Fig. 8 – (a) Cascades of S-MFCs powering LEDs. (b) Change in Voltage and Current with time during cascade operation of MFCs to power 3 LEDs. (c) operating resistance of the LEDs.

other applications. In advance, the effect of cascading the MFCs at different electrode spacing was tested. At the point where the MFCs had very close OCV values (0.817 ± 0.04 V), they were connected in series to power light-emitting diodes (LEDs) connected in parallel (Fig. 8).

Before the red LEDs were connected, MFC_2 h, MFC_5 h, and MFC_8 h had OCVs of 0.818 V, 0.849 V, and 0.831 V, respectively, while the measured output voltage when the three MFCs were connected in series was 2.498 V. Similarly, before the green LEDs were cascaded, the duplicates had 0.724 V, 0.826 V, and 0.851 V, respectively, while the measured output voltage when connected in series was 2.401 V. The change in voltage and current when three LEDs were connected is shown in Fig. 8 (b), while Fig. 8 (c) shows the change in the LEDs' resistance with time. The red LEDs drew a higher current due to lower resistance and were therefore operated at a lower voltage than the green LEDs, which had a higher voltage and lower current due to higher resistance. After the initial drop, the voltage across the LEDs was stable.

One of the desirable characteristics of MFCs in scale-up studies is their compatibility in cascade operation since most MFC stacks are associated with voltage or current reversal [37] in the fed-batch process [60]. The output voltage resulting from the series connection of the MFCs in this study was the sum of the voltages of the individual MFCs. This shows that electrode spacing is not a constraint when similar S-MFCs built with the same electrode materials are electrically connected and operated in series in a single chamber configuration. This synergistic performance of the MFCs at different electrode spacings in a series connection without voltage reversal establishes the S-MFC as one of the most promising bio-electrochemical systems, which can be scaled up for real applications. Moreover, it can be inferred from Fig. 8(b) that voltage stability can be achieved with the S-MFC at actual external loads. The large current drop when the LEDs were connected shows that the MFC's architectural and biological optimization is still necessary to improve the current density.

Conclusions

This study highlighted the importance of anode-cathode spacing on the long-term performance of a soil MFC fed with urine as a substrate. The study showed that the performance stability of the S-MFC was time-dependent on the electrode spacing. At the beginning of feeding, electrode spacing of 2 cm showed the best performance due to lower internal resistance and the immediate availability of the substrate at the anode for microbial metabolism. More extended feeding resulted in better performance and power stability at 5 cm and 8 cm electrode spacing, respectively, with 8 cm yielding the overall best performance (271.1 ± 11.3 mW/m² at a current density of 600.4 ± 23.1 mA/m²) toward the end of the experiment. These results showed that the long-term operation of an S-MFC in fed-batch mode is possible without changing the medium and electrodes. It was also shown that in the fed-batch process with urine, a larger electrode gap is required for long-term feeding to maintain the maximum performance of the S-MFC.

These results are very crucial for the long-term in-situ deployment of the S-MFC. While significant improvement was achieved with the fed-batch operation of the MFC at varying electrode spacing, it is evident that a feeding frequency of 6 days is not optimal for performance. The intermittent loss of performance observed at some sites with more prolonged

feeding also deserves further investigation. Therefore, other studies are needed to investigate the response of the microbial community to the treatments. The effect of the interaction between electrode spacing and feeding frequency on the performance of the S-MFC configuration used in this study also merits further investigation.

Declaration of competing interest

The authors declare that they have no known competing financial interests or personal relationships that could have appeared to influence the work reported in this paper.

Acknowledgements

This study was supported by the Petroleum Technology Development Fund (PTDF), Nigeria, and the German Academic Exchange Service (DAAD) within the Nigerian-German Postgraduate Program 2018; while the Chair of Process Biotechnology, University of Bayreuth, Germany, provided the materials and the working environment in collaboration with Center for Energy Technology- Technologie Allianz Oberfranken (ZET-TAO).

Appendix A. Supplementary data

Supplementary data to this article can be found online at <https://doi.org/10.1016/j.ijhydene.2021.11.110>.

REFERENCES

- [1] Dincer I, Acar C. Review and evaluation of hydrogen production methods for better sustainability. *Int J Hydrogen Energy* 2015;40(34):11094–111. <https://doi.org/10.1016/j.ijhydene.2014.12.035>.
- [2] Bocci E, Di Carlo A, McPhail SJ, Gallucci K, Foscolo PU, Moneti M, et al. Biomass to fuel cells state of the art: a review of the most innovative technology solutions. *Int J Hydrogen Energy* 2014;39(36):21876–95. <https://doi.org/10.1016/j.ijhydene.2014.09.022>.
- [3] Dincer I. Environmental and sustainability aspects of hydrogen and fuel cell systems. *Int J Energy Res* 2007;31(1):29–55. <https://doi.org/10.1002/er.1226>.
- [4] Seyhan M, Akansu YE, Murat M, Korkmaz Y, Akansu SO. Performance prediction of PEM fuel cell with wavy serpentine flow channel by using artificial neural network. *Int J Hydrogen Energy* 2017;42(40):25619–29. <https://doi.org/10.1016/j.ijhydene.2017.04.001>.
- [5] Singh D, Pratap D, Baranwal Y, Kumar B, Chaudhary RK. Microbial fuel cells: a green technology for power generation. *Ann Biol Res* 2010;1(3):128–38.
- [6] Lincy M, Kumar B, Vasantha V, Varalakshmi P. Microbial fuel cells: a promising alternative energy source. In: Krishnaraj R, Yu J-S, editors. *Bioenergy*. Apple Academic Press; 2015. p. 61–85.
- [7] Rahimnejad M, Adhami A, Darvari S, Zirepour A, Oh S-E. Microbial fuel cell as new technology for bioelectricity generation: a review. *Alexandria Engineering Journal* 2015;54(3):745–56. <https://doi.org/10.1016/j.aej.2015.03.031>.
- [8] Hernández-Flores G, Poggi-Varaldo HM, Solorza-Feria O, Romero-Castañón T, Ríos-Leal E, Galíndez-Mayer J, et al. Batch operation of a microbial fuel cell equipped with alternative proton exchange membrane. *Int J Hydrogen Energy* 2015;40(48):17323–31. <https://doi.org/10.1016/j.ijhydene.2015.06.057>.
- [9] Song T-S, Wang D-B, Han S, Wu X-y, Zhou CC. Influence of biomass addition on electricity harvesting from solid phase microbial fuel cells. *Int J Hydrogen Energy* 2014;39(2):1056–62. <https://doi.org/10.1016/j.ijhydene.2013.10.125>.
- [10] Jadhav DA, Mungray AK, Arkatkar A, Kumar SS. Recent advancement in scaling-up applications of microbial fuel cells: from reality to practicability. *Sustain Energy Technol and Assessments* 2021;45:101226. <https://doi.org/10.1016/j.seta.2021.101226>.
- [11] Pandit S, Savla N, Jung SP. Recent advancements in scaling up microbial fuel cells. In: Abbassi R, editor. *Integrated microbial fuel cells for wastewater treatment*. Waltham: Elsevier; 2020. p. 349–68.
- [12] Adekunle A, Raghavan V, Tartakovsky B. Carbon source and energy harvesting optimization in solid anolyte microbial fuel cells. *J Power Sources* 2017;356:324–30. <https://doi.org/10.1016/j.jpowsour.2017.01.062>.
- [13] Wang H, Park J-D, Ren ZJ. Practical energy harvesting for microbial fuel cells: a review. *Environ Sci Technol* 2015;49(6):3267–77. <https://doi.org/10.1021/es5047765>.
- [14] Abbas SZ, Rafatullah M. Recent advances in soil microbial fuel cells for soil contaminants remediation. *Chemosphere* 2021;129691. <https://doi.org/10.1016/j.chemosphere.2021.129691>.
- [15] Li X, Wang X, Zhao Q, Zhang Y, Zhou Q. In situ representation of soil/sediment conductivity using electrochemical impedance spectroscopy. *Sensors* 2016;16(5). <https://doi.org/10.3390/s16050625>.
- [16] Bose D, Dey A, Banerjee T. Aspects of bioeconomy and microbial fuel cell technologies for sustainable development. *Sustainability* 2020;13(3):107–18. <https://doi.org/10.1089/sus.2019.0048>.
- [17] Simeon I OAR, Gbabo A, Okoro-Shekwa C. Performance of a single chamber soil microbial fuel cell at varied external resistances for electric power generation. *J Renewable Energy and Environ* 2016;3(3). <https://doi.org/10.30501/jree.2016.70092>.
- [18] Simeon MI, Otache MY, i Ewemojie TA, Raji AO. Application of urine as fuel in a soil-based membrane-less single chamber microbial fuel cell. *AgricEngInt: CIGR Journal* 2019;21(1):115–21.
- [19] Simeon MI, Raji AO. Experimental utilization of urine to recharge soil microbial fuel cell for constant power generation. *Res J Eng and Environ Sci* 2016;1(1):129–35.
- [20] Hassan SHA, Gad El-Rab SMF, Rahimnejad M, Ghasemi M, Joo J-H, Sik-Ok Y, et al. Electricity generation from rice straw using a microbial fuel cell. *Int J Hydrogen Energy* 2014;39(17):9490–6. <https://doi.org/10.1016/j.ijhydene.2014.03.259>.
- [21] Simeon MI, Asoiro FU, Aliyu M, Raji OA, Freitag R. Polarization and power density trends of a soil-based microbial fuel cell treated with human urine. *Int J Energy Res* 2020;44(7):5968–76. <https://doi.org/10.1002/er.5391>.
- [22] Kumar S, Magotra VK, Jeon HC, Kang TW, Inamdar AI, Aqueel AT, et al. Multifunctional ammonium fuel cell using compost as a novel electro-catalyst. *J Power Sources* 2018;402:221–8. <https://doi.org/10.1016/j.jpowsour.2018.09.041>.

- [23] Magotra VK, Kumar S, Kang TW, Inamdar AI, Aqueel AT, Im H, et al. Compost soil microbial fuel cell to generate power using urea as fuel. *Sci Rep* 2020;10(1):4154. <https://doi.org/10.1038/s41598-020-61038-7>.
- [24] Pinto D, Coradin T, Laberty-Robert C. Effect of anode polarization on biofilm formation and electron transfer in *Shewanella oneidensis*/graphite felt microbial fuel cells. *Bioelectrochemistry* 2018;120:1–9. <https://doi.org/10.1016/j.bioelechem.2017.10.008>.
- [25] Cheng L, Di Min, Liu D-F, Zhu T-T, Wang K-L, Yu H-Q. Deteriorated biofilm-forming capacity and electroactivity of *Shewanella oneidensis* MR-1 induced by insertion sequence (IS) elements. *Biosens Bioelectron* 2020;156:112136. <https://doi.org/10.1016/j.bios.2020.112136>.
- [26] Yang Y-C, Chen C-C, Huang C-S, Wang C-T, Ong H-C. Developments of metallic anodes with various compositions and surfaces for the microbial fuel cells. *Int J Hydrogen Energy* 2017;42(34):22235–42. <https://doi.org/10.1016/j.ijhydene.2017.05.096>.
- [27] Jung S, Regan JM. Comparison of anode bacterial communities and performance in microbial fuel cells with different electron donors. *Appl Microbiol Biotechnol* 2007;77(2):393–402. <https://doi.org/10.1007/s00253-007-1162-y>.
- [28] Franks AE, Nevin KP. Microbial fuel cells, A current review. *Energies* 2010;3(5):899–919. <https://doi.org/10.3390/en3050899>.
- [30] Liu H, Cheng S, Logan BE. Power generation in fed-batch microbial fuel cells as a function of ionic strength, temperature, and reactor configuration. *Environ Sci Technol* 2005;39(14):5488–93. <https://doi.org/10.1021/es050316c>.
- [31] Chouler J, Bentley I, Vaz F, O'Fee A, Cameron PJ, Di Lorenzo M. Exploring the use of cost-effective membrane materials for Microbial Fuel Cell based sensors. *Electrochim Acta* 2017;231:319–26. <https://doi.org/10.1016/j.electacta.2017.01.195>.
- [32] Lee C-Y, Huang Y-N. The effects of electrode spacing on the performance of microbial fuel cells under different substrate concentrations. *Water Sci Technol* 2013;68(9):2028–34. <https://doi.org/10.2166/wst.2013.446>.
- [33] Lefebvre O, Uzabiaga A, Shen YJ, Tan Z, Cheng YP, Liu W, et al. Conception and optimization of a membrane electrode assembly microbial fuel cell (MEA-MFC) for treatment of domestic wastewater. *Water Sci Technol* 2011;64(7):1527–32. <https://doi.org/10.2166/wst.2011.067>.
- [34] Kang H, Jeong J, Gupta PL, Jung SP. Effects of brush-anode configurations on performance and electrochemistry of microbial fuel cells. *Int J Hydrogen Energy* 2017;42(45):27693–700. <https://doi.org/10.1016/j.ijhydene.2017.06.181>.
- [35] Kuntke P, Smiech KM, Bruning H, Zeeman G, Saakes M, Sleutels THJA, et al. Ammonium recovery and energy production from urine by a microbial fuel cell. *Water Res* 2012;46(8):2627–36. <https://doi.org/10.1016/j.watres.2012.02.025>.
- [36] Bagchi S, Behera M. Microbial fuel cells. In: Navanietha Krishnaraj R, Sani RK, editors. *Bioelectrochemical interface engineering*. Hoboken, NJ: Wiley; 2020. p. 91–116.
- [37] Nam T, Kang H, Pandit S, Kim S-H, Yoon S, Bae S, et al. Effects of vertical and horizontal configurations of different numbers of brush anodes on performance and electrochemistry of microbial fuel cells. *J Clean Prod* 2020;277:124125. <https://doi.org/10.1016/j.jclepro.2020.124125>.
- [38] Pietrelli A, Micangeli A, Ferrara V, Raffi A. Wireless sensor network powered by a terrestrial microbial fuel cell as a sustainable land monitoring energy system. *Sustainability* 2014;6(10):7263–75. <https://doi.org/10.3390/su6107263>.
- [39] Barbato RA, Foley KL, Toro-Zapata JA, Jones RM, Reynolds CM. The power of soil microbes: sustained power production in terrestrial microbial fuel cells under various temperature regimes. *Appl Soil Ecol* 2017;109:14–22. <https://doi.org/10.1016/j.apsoil.2016.10.001>.
- [40] Dunaj SJ, Vallino JJ, Hines ME, Gay M, Kobyljanec C, Rooney-Varga JN. Relationships between soil organic matter, nutrients, bacterial community structure, and the performance of microbial fuel cells. *Environ Sci Technol* 2012;46(3):1914–22. <https://doi.org/10.1021/es2032532>.
- [41] Jiang Y-B, Zhong W-H, Han C, Deng H. Characterization of electricity generated by soil in microbial fuel cells and the isolation of soil source exoelectrogenic bacteria. *Front Microbiol* 2016;7:1776. <https://doi.org/10.3389/fmicb.2016.01776>.
- [42] Im S-W, Lee H-J, Chung J-W, Ahn Y-T. The effect of electrode spacing and size on the performance of soil microbial fuel cells (SMFC). *J Korean Society of Environ Engineers* 2014;36(11):758–63. <https://doi.org/10.4491/KSEE.2014.36.11.758>.
- [43] Simeon I.M., Imoize A.L., Freitag R. Evaluation of the electrical performance of a soil-type microbial fuel cell treated with a substrate at different electrode spacings. In: International conference on energy, environment and storage, p. 430–435.
- [44] Meshack Simeon I, Imoize AL, Freitag R. Comparative evaluation of the performance of a capacitive and a non-capacitive microbial fuel cell. In: 2021 18th international multi-conference on systems, signals & devices (SSD), 2021 - 2021. p. 1076–82. <https://doi.org/10.1109/SSD52085.2021.9429481>.
- [45] Liang Y, Feng H, Shen D, Li N, Guo K, Zhou Y, et al. Enhancement of anodic biofilm formation and current output in microbial fuel cells by composite modification of stainless steel electrodes. *J Power Sources* 2017;342:98–104. <https://doi.org/10.1016/j.jpowsour.2016.12.020>.
- [46] Karra U, Muto E, Umaz R, Kölln M, Santoro C, Wang L, et al. Performance evaluation of activated carbon-based electrodes with novel power management system for long-term benthic microbial fuel cells. *Int J Hydrogen Energy* 2014;39(36):21847–56. <https://doi.org/10.1016/j.ijhydene.2014.06.095>.
- [47] Sherafatmand M, Ng HY. Using sediment microbial fuel cells (SMFCs) for bioremediation of polycyclic aromatic hydrocarbons (PAHs). *Bioresour Technol* 2015;195:122–30. <https://doi.org/10.1016/j.biortech.2015.06.002>.
- [48] Haddadi S, Nabi-Bidhendi G, Mehrdadi N. Nitrogen removal from wastewater through microbial electrolysis cells and cation exchange membrane. *J Environ Health Sci Eng* 2014;12(1):48. <https://doi.org/10.1186/2052-336X-12-48>.
- [49] Walter XA, Santoro C, Greenman J, Ieropoulos I. Self-stratifying microbial fuel cell: the importance of the cathode electrode immersion height. *Int J Hydrogen Energy* 2019;44(9):4524–32. <https://doi.org/10.1016/j.ijhydene.2018.07.033>.
- [50] Nam T, Son S, Koo B, Hoa Tran HV, Kim JR, Choi Y, et al. Comparative evaluation of performance and electrochemistry of microbial fuel cells with different anode structures and materials. *Int J Hydrogen Energy* 2017;42(45):27677–84. <https://doi.org/10.1016/j.ijhydene.2017.07.180>.
- [51] Khater Dena, El-khatib KM, Hazaa M, Hassan Rabeay YA. Activated sludge-based microbial fuel cell for bio-electricity generation. *J Basic and Environ Sci* 2015;2:63–73.
- [52] Khater DZ, El-Khatib KM, Hassan HM. Microbial diversity structure in acetate single chamber microbial fuel cell for electricity generation. *J Genet Eng Biotechnol* 2017;15(1):127–37. <https://doi.org/10.1016/j.jgeb.2017.01.008>.
- [53] Ray H, Saetta D, Boyer TH. Characterization of urea hydrolysis in fresh human urine and inhibition by chemical

- addition. *Environ Sci: Water Res. Technol.* 2018;4(1):87–98. <https://doi.org/10.1039/C7EW00271H>.
- [54] Velasquez-Orta SB, Yu E, Katuri KP, Head IM, Curtis TP, Scott K. Evaluation of hydrolysis and fermentation rates in microbial fuel cells. *Appl Microbiol Biotechnol* 2011;90(2):789–98. <https://doi.org/10.1007/s00253-011-3126-5>.
- [55] Kim MH, Iwuchukwu IJ, Wang Y, Shin D, Sanseverino J, Frymier P. An analysis of the performance of an anaerobic dual anode-chambered microbial fuel cell. *J Power Sources* 2011;196(4):1909–14. <https://doi.org/10.1016/j.jpowsour.2010.09.064>.
- [56] Ebuka Igboamalu Tony, Niel Bezuidenhout, Mpumelelo Thomas Matsena, Chirwa Evans MN. Microbial fuel cell power output and growth: effect of pH on anaerobic microbe consortium. *Chem Eng Transactions* 2019;76:1381–6. <https://doi.org/10.3303/CET1976231>.
- [57] Magotra VK, Kang TW, Lee SJ, Walke PD, Rana AuHS, Jeon HC. Urea - hydrogen compost soil microbial fuel cell for multifunctional applications. 2020.
- [58] Xia X, Tokash JC, Zhang F, Liang P, Huang X, Logan BE. Oxygen-reducing biocathodes operating with passive oxygen transfer in microbial fuel cells. *Environ Sci Technol* 2013;47(4):2085–91. <https://doi.org/10.1021/es3027659>.
- [59] Xiu S, Yao J, Wu G, Huang Y, Yang B, Huang Y, et al. Hydrogen-mediated electron transfer in hybrid microbial–inorganic systems and application in energy and the environment. *Energy Technol* 2019;7:1–8. <https://doi.org/10.1002/ente.201800987>.
- [60] Oh S-E, Logan BE. Voltage reversal during microbial fuel cell stack operation. *J Power Sources* 2007;167(1):11–7. <https://doi.org/10.1016/j.jpowsour.2007.02.016>.